Journal of Molecular Liquids 376 (2023) 121464

Contents lists available at ScienceDirect

Journal of Molecular Liquids

journal homepage: www.elsevier.com/locate/molliq

Preparation and thermophysical characterisation analysis of potential nano-phase transition materials for thermal energy storage applications

Muhammad Aamer Hayat [a,*], Yongzhen Yang [b], Liang Li [a], Mose Bevilacqua [a], Yongkang Chen [a,*]

[a] School of Physics, Engineering and Computer Science, University of Hertfordshire, Hatfield, Herts, AL10 9AB, United Kingdom
[b] Key Laboratory of Interface Science and Engineering in Advanced Materials, Ministry of Education, Taiyuan University of Technology, Taiyuan, Shanxi, China

ARTICLE INFO

Article history:
Received 17 November 2022
Revised 3 February 2023
Accepted 11 February 2023
Available online 14 February 2023

Keywords:
Nano phase change material
Nanofiller
Thermal conductivity
Latent heat
Energy storage

ABSTRACT

The efficacious use of phase change materials (PCMs) is mainly confined by their poor thermal conductivity (TC). In this study, multiwalled carbon nanotubes (MWCNTs), graphene nanoplatelets (GNP) and titanium oxide (TiO_2) based single, and novel hybrid nano additives were incorporated into paraffin, a typical PCM, to find the optimal composite which could not only enhance the thermal conductivity but also limit the latent heat. Both unitary and hybrid nanoparticles at five different concentrations (0.2, 0.4, 0.6, 0.8 & 1.0 wt%) were investigated using various characterisation techniques, including FT-IR, XRD, DSC, TGA, and TC apparatus. The results depicted good intermolecular interactions between the PCM and the nanoparticles and showed that the dispersion of nanoparticles within the PCM did not affect the chemical structure of pristine paraffin but enhanced its thermal and chemical stability. Novel hybrid nanocomposites were found to be more stable and exhibit better thermal performance than single nanocomposites. The highest value of thermal conductivity was observed at 1.0 wt% of GNP + MWCNTs hybrid particles based PCM with a maximum enhancement of 170% at 25 °C. However, compared with single and hybrid carbon-based nanofillers, TiO_2 based mono and hybrid nano-PCM showed a minimum reduction in the latent heat with a maximum decrease of −3.7%, −5.2%, and −5.5% at 1 wt% of TiO_2, TiO_2 + GNP and TiO_2 + MWCNTs, respectively. The significant improvement in the thermal properties of PCMs with the inclusion of these nanofillers indicates that they have the potential to be employed in thermal energy storage applications.

1. Introduction

The energy crisis is a significant issue in the modern world owing to enormous population growth and a high rise in energy consumption [1]. Although researchers have considered and established renewable energy sources, such as wind and solar, to replace traditional fossil fuel energy resources, optimising the present use of energy should not be ignored. It is essential to understand how to preserve and maximise energy use before incorporating renewable energy. One strategy to conserve excess energy is using thermal energy storage materials. Instead of releasing it into the atmosphere, thermal energy can be preserved for subsequent use [2,3].

Phase change materials (PCMs) provide impressive thermal storage characteristics because they can store and discharge significant quantities of latent heat. However, PCMs suffer from low thermal conductivity (TC), which results in poor heat transfer performance. Many TC enhancement techniques have been investigated by several researchers to improve their TC values, such as metal foams [4], fins [5], heat pipes [6], and nanofillers [7]. Recent review articles [8–13] have suggested that the use of nanoparticles instead of bulky metals has good potential to improve the thermophysical properties of PCMs since nanoparticles retain high TC, low density, together with high specific surface area and they also have good compatibility with PCMs. It has been reported that carbon-based nanofillers (CNTs, GNP, diamond, and graphene flakes) have a higher thermal conductivity enhancement compared to metals (Cu, Al, Ag, Fe, Ni), and metallic oxides (TiO_2, Al_2O_3, CuO, Fe_3O_4, MgO, SiO_2, ZnO) nanoparticles [8–10]. For instance, Fan et al. [11] incorporated different carbon nanoparticles in paraffin with a mass concentration between 1 and 5 wt%. They found that the thermal conductivity of the PCM with the addition of 5 wt% of GNPs was increased by 164% with a slight decrease in the energy storage capacity. Arshad et al. [12] used 1 wt% of MWCNTs, GNP, GO and rGO with paraffin as the PCM. The results showed an increase of 66%, 77%, 74.9% and 77.7% in TC by the addition of MWCNTs,

* Corresponding authors.
E-mail addresses: m.hayat2@herts.ac.uk (M.A. Hayat), y.k.chen@herts.ac.uk (Y. Chen).

https://doi.org/10.1016/j.molliq.2023.121464
0167-7322/

Nomenclature

Abbreviations

LHTESS	Latent heat thermal energy storage system
MWCNTs	Multiwalled carbon nanotubes
TiO_2	Titanium oxide
GNP	Graphene nanoplatelets
TC	Thermal conductivity
PAR	Paraffin
GO	Graphene oxide
SDBS	Sodium dodeecycl-benzene
xGnP	Exfoliated Graphite Nanoplatelets
PCM	Phase change material
S-MWCNTs	Small-Multi wall carbon nanotubes
Al	Aluminium
Ag	Silver
Fe	Iron
Ni	Nickel
Al_2O_3	Aluminium oxide
CuO	Copper oxide
Fe_3O_4	Iron oxide
MgO	Magnesium oxide
SiO_2	Silicon dioxide
ZnO	Zinc oxide
Cu	Copper

Symbols

T_{peak}	Peak melting temperature
ΔH	Latent heat
ΔT	Degree of super cooling
wt.%	Mass fraction of nanoparticles
RE	Relative error
K	Thermal conductivity

GNP, GO and rGO nanoparticles, respectively, and less than 10% decrease in the heat storage capacity for all composites. Dixit et al. [13] analysed expanded graphite and PCM based composites and observed very good thermal stability after 250 thermal cycles with only a 6% decrease in melting and solidification enthalpies. Harish et al. [14] studied the influence of GnP on the thermal conductivity of lauric acid as their PCM and noticed that the incorporation of 1 vol% of GnP into lauric acid raised its thermal conductivity by 230%. The thermal conductivity of lauric acid was greatly improved by the graphene nanoplatelets without affecting their phase transition enthalpy and melting temperature. In their another study [15], they investigated different types of carbon-based nano additives (i.e., SWCNTs, MWCNTs and graphene nanosheets) with n-dodecanoic acid as their PCM. The experimental results showed that the thermal conductivity in the solid state was increased by 223%, 171% and 27%, while in the liquid state it was enhanced by 39%, 19.8% and 4% with the inclusion of graphene nanosheets, MWCNTs and SWCNTs, respectively. The graphene nanosheets showed a remarkable improvement because of their high aspect ratio and less interface thermal resistance compared to other carbon nano inclusions. In addition, due to higher interfacial thermal resistance in the liquid state than in the solid state, the thermal conductivity enhancement ratio was lower in liquids. Wang et al. [16] incorporated various concentrations of graphene in the PCM (n-hexadecane) and discovered a linear increase in thermal conductivity with no effect on the PCM's thermal performance. Bahiraei et al. [17] examined several types of carbon-based nanofillers at four different concentrations and found that a dispersion of 10 wt% graphite nanoparticles improved TC significantly with a slight depreciation in latent heat. Recently, Chinnasamy and Cho [18] varied the MWCNTs concentrations from 1 wt% to 5 wt% to find the optimum concentration for lauryl alcohol organic PCM. They found that at 3 wt% of MWCNTs the thermal conductivity was improved by 41%, 77.8% and 74.6% at 10, 30 and 40 °C, respectively. Lower latent heat values and increased supercooling behaviour was observed when the concentration was increased beyond 3 wt%. The aforementioned studies report that the inclusion of highly thermally conductive carbon nanoparticles significantly improves the thermal conductivity of PCMs with a minimal reduction in latent heat values [19,20]. However, the latest studies have shown that the problems of stability and the high cost of carbon-based nano-additives in PCMs have not been solved yet. In particular, MWCNTs do not disperse into PCMs properly due to their hydrophobic nature, which causes a stability problem for nano PCMs [21–24]. Therefore, it is necessary to find low-cost alternatives to expensive nanomaterials with a minimal effect on the overall thermophysical properties of nano-PCMs. There are very few studies in which hybrid nanoparticles were used with PCMs, and there are no studies in which two different families of hybrid nanoparticles have been used with PCMs [25–29]. Furthermore, scientists have reported that hybrid nanomaterials could be advantageous due to their exceptional thermophysical characteristics, which allow them to be used in a variety of applications to reduce costs and improve efficacy [30,31]. From the literature [25,32], it was found that TiO_2 particles have good stability, and have a relatively limited impact on latent heat reduction because of their good stability and intermolecular interactions with PCM molecules. Additionally, TiO_2 particles are less expensive than other inorganic particles including Ag, Cu, CuO, B_2O_3, Fe_3O_4, and SiO_2 [33–35].

This study presents an investigation of an organic PCM incorporated with carbon and metal oxide-based single and hybrid nanofillers (GNP, MWCNTs, TiO_2, GNP + MWCNTs, GNP + TiO_2 and MWCNTs + TiO_2) at five different concentrations (0.2 wt%, 0.4 wt %, 0.6 wt%, 0.8 and 1.0 wt%) to identify the optimum combination with lower cost, good stability and thermophysical characteristics. The current experimental work employs various characterisation techniques to investigate the thermal conductivity, chemical structure, thermal stability, crystal structure and important thermal properties, and new findings are reported.

2. Experimental stages

2.1. Materials

Paraffin (PAR) with a nominal melting temperature range of 27–29 °C was utilised as a PCM and was provided by Rubitherm GmbH, Germany. This specific PCM with a melting temperature range of 27–29 °C was selected for its proximity to the nominal indoor comfort temperature of buildings and its versatility for use in other thermal energy storage applications within that temperature range. The thermophysical characteristics of paraffin are presented in Table 1. Three distinct types of nanofillers TiO_2, GNP and MWCNTs were chosen to improve the PCM's thermal conductivity and were provided by Sigma-Aldrich, UK. Anatase TiO_2 nanoparticles with 99.7% trace metal basis had particle size less than 25 nm,

Table 1
PCM thermal properties.

PCM	Melting temperature (°C)	Heat storage capacity (kJ/Kg)	Specific heat capacity (kJ/Kg)	Thermal conductivity (W/m. K)	Density (kg/m^3)
Paraffin	27–29	250	2	0.2	880 at 15 °C 770 at 40 °C

density of 3.9 g/mL, and surface area of 45–55 m^2/g at 25 °C. GNP with particle size less than 2 μm had surface area of 750 m^2/g and MWCNTs with an outer diameter range of 6–13 nm, a length range of 2.5–20 μm, surface area of 220 m^2/g, 98% trace metals basis, density of 2.1 g/mL at 25 °C. Transmission electron microscopy (TEM) was used to examine the surface structures of nanoparticles, as shown in Fig. 1. In addition, sodium dodecylbenzene sulfonate (SDBS) was used as a surfactant and was obtained from Sigma-Aldrich, UK. All employed materials were utilised without any chemical alteration.

2.2. Preparation of nano-PCMs

For the preparation of nano-enhanced phase change materials (nano-PCMs) a two-step protocol was used, which has been widely employed in the fabrication of nanofluids [36]. Five different concentrations (0.2, 0.4, 0.6, 0.8, and 1 wt%) of TiO_2, GNP and MWCNTs for both mono and hybrid nano-PCMs were impregnated into the base PCM. The schematic diagram of the two-step method used for the preparation of mono and hybrid nano-enhanced PCMs is shown in Fig. 2. Furthermore, for each concentration of TiO_2, GNP, and MWCNT nanofillers, 25% of sodium dodecylbenzene sulfonate (SDBS) was incorporated. The mass concentration ratio of hybrid nano-PCMs (TiO_2/MWCNT, TiO_2/GNP and GNP/MWCNT) was held at 70%/30% of 0.2, 0.4, 0.6, 0.8 and 1.0 wt%. For the TiO_2 based hybrid particles (i.e., TiO_2/MWCNT and TiO_2/GNP), 70% of the TiO_2 particles were used since they have better stability, and less impact on latent heat because of their good intermolecular interactions with the base PCM, and they are also economical [37].

Firstly, paraffin was melted in a thermal bath at a constant temperature of 60 °C and then a fixed amount of nanofillers were introduced into a certain quantity of PCM. To obtain a homogeneous solution and to break up the particle clusters, a magnetic stirrer was used for 2.5 h at 500 rpm at 60 °C to stir and homogenise the mixture. Subsequently, SDBS was added separately into the mixture and further stirring continued for half an hour to ensure better dispersion of nanoparticles in the PCM since SDBS has good hydrophilicity, which significantly decreases the surface tension of PCM during the nano-PCM preparation. Secondly, all samples were sonicated for 45 min utilising a probe sonicator at a 40% amplitude and 20 kHz frequency to enhance the dispersion and homogeneity of the nanofillers while minimising aggregation and sedimentation. Lastly, all the nano-PCM samples were cooled to a room temperature of 20 °C.

Images of the freshly prepared samples and the samples left in a hot water bath at 60 °C for 48 h are shown in Fig. 3 (a – d). Apart from the single MWCNT nanoparticles based PCM a uniform dispersion after 48 h of sonication of mono and hybrid nano-PCMs was observed. As shown in Fig. 3b, MWCNTs settled down after 48 h when they were incorporated in the PCM, since the hydropho-

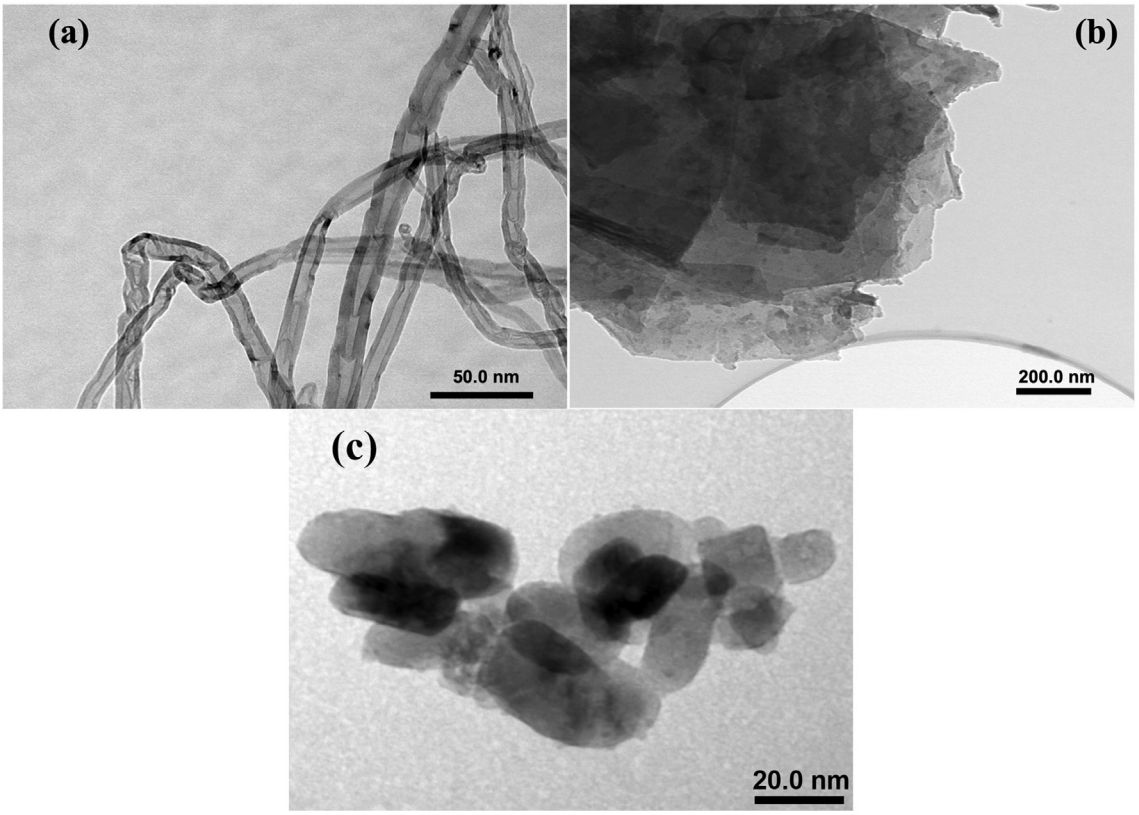

Fig. 1. Typical TEM images of (a) MWCNTs, (b) GNP, and (c) TiO_2.

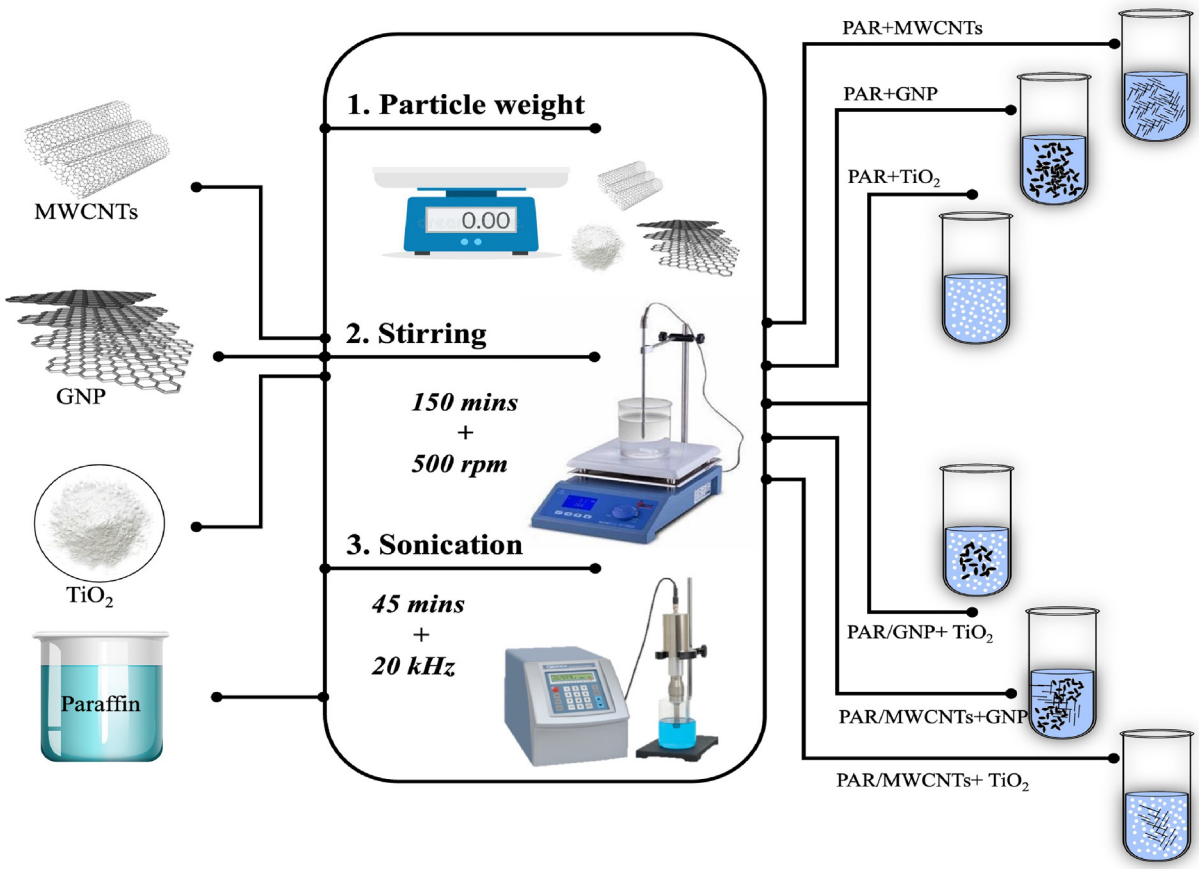

Fig. 2. Schematic illustration of the two-step method.

bic nature of MWCNTs prevents them from dispersing uniformly in the PCM. MWCNTs-based hybrid composites, on the other hand, demonstrated a uniform dispersion after 48 h due to the small amount (i.e., 30%) of MWCNTs used in the hybrid composites and their good interactions with TiO_2 and GNP particles.

2.3. Characterisation

A range of characterisation methods have been used to investigate the structural and chemical properties of the base PCM, and nanoparticle enhanced PCMs. These characterisation techniques include FTIR, XRD, DSC, TGA, and TC apparatus.

A Fourier transform infrared spectroscope (FTIR, Perkin Elmer Frontier) was employed to investigate the absorption spectra and chemical structure of the nano-PCMs at room temperature. The FTIR experiments were carried out at wavelengths ranging from 600 to 4000 cm^{-1}, with a spectral resolution and accuracy of 4 cm^{-1} and 0.01 cm^{-1}, respectively. X-ray diffractometer (XRD) using Cu-Kα X-ray radiation was provided by Bruker, UK and employed to study the crystalline structures of the base PCM and composite PCMs within the 2θ range of 5-60°.

The thermal stability, thermal conductivity, and latent heat of melting and solidification were among the measured thermal parameters of the composite PCMs. Differential scanning calorimetry (DSC-Q200, TA Instrument Inc., UK) was utilised to investigate the melting, crystallisation temperature and latent heat of pure paraffin and composite paraffin enhanced with nanofillers over the temperature range of 5 – 55 °C at a heating and cooling rate of 1 °C min^{-1} under an N_2 atmosphere. Before the experiments, the DSC was calibrated by measuring the ΔH_{fusion} and T_{onset} of high purity standard indium (ΔH_{fusion} = 28.7 Jg^{-1} and T_{onset} = 156.6 °C) samples. Thermal stability of the pure PCM and nano-PCMs was tested by thermogravimetric analysis (TGA, TGA Q-50, TA instrument Inc., UK) and derivative thermogravimetry (DTG) between 40 and 400 °C at a heating rate of 10 °C min^{-1} under a nitrogen purge flow rate of 100 mL min^{-1} [38]. A modulated differential scanning calorimeter was used to determine the specific heat capacity of samples (MDSC; Q200, TA Instruments, Inc.). The MDSC generated Cp data with an accuracy of up to ± 2%. The samples were placed in a DSC apparatus using a Tzero hermetic pan and lid (TA Instruments). The sample mass ranged between 10 and 15 mg. To perform the heat capacity measurements with the MDSC, a standard automated procedure was applied. The samples were heated between 10 °C and 55 °C at a heating rating rate of 2 °C.min^{-1}. A Hot Disk Thermal Constant Analyzer (TPS-2500S) was employed to determine the thermal conductivity of the PCM and nano-PCM samples. The technique is standardised in ISO 22007-2. Fig. 4 depicts the thermal conductivity setup with the sample holder's design, which includes six channels at the bottom for effective heat transmission. A new aluminium sample holder was fabricated and placed inside the heat immersion circulator to evaluate thermal conductivity at different temperatures. Since the manufacturer's testing holder is confined to room temperature measurements, this sample holder was developed according to the TPS 2500S manufacturer's recommendations to test PCMs at various temperatures other than room temperature. To raise the temperature of the sample, the Hot Disk sensor 5465 (3.089 mm radius) was used, which consisted of a double spiral thin metal foil sandwiched between two thin sheets of insulating Teflon material. In addition, hot disk equipment was calibrated with the stainless-

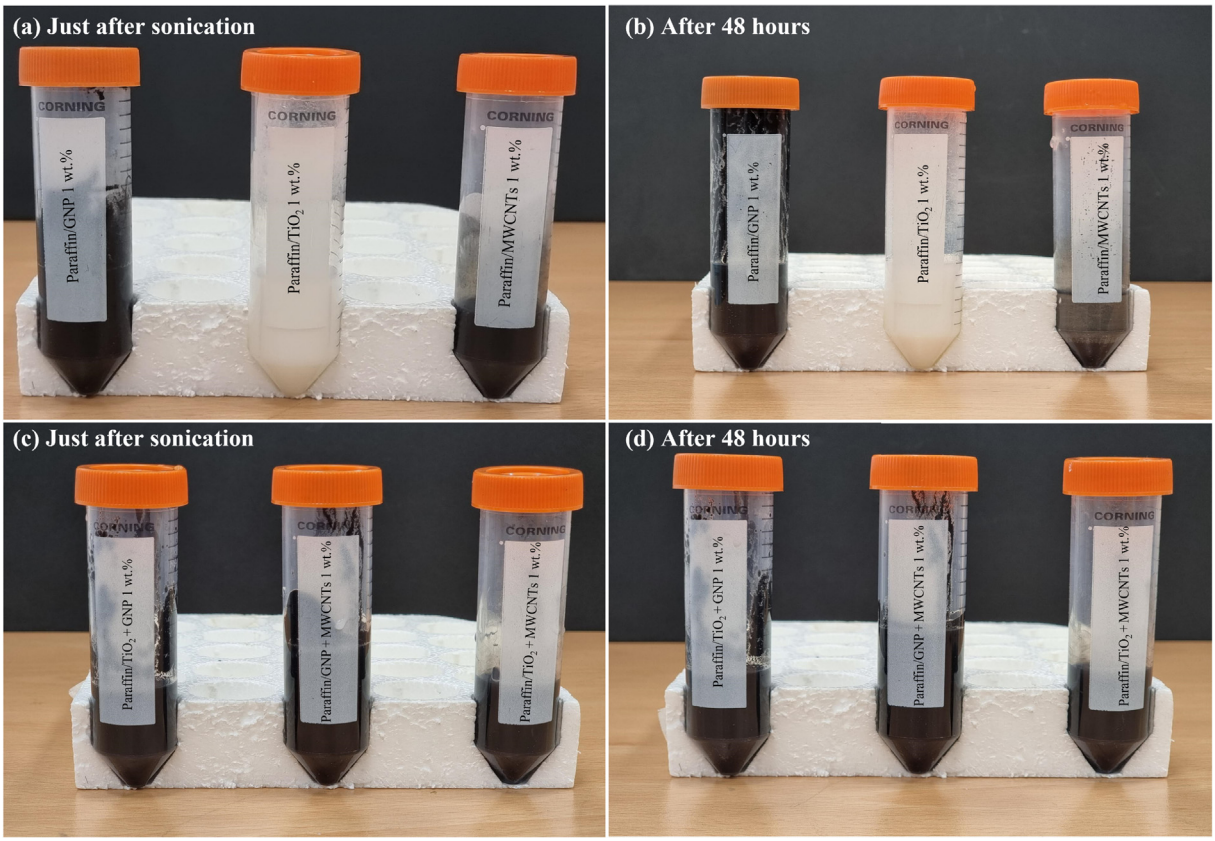

Fig. 3. Status of samples with a time duration. (a) Single type particles-based nanocomposites just after sonication, (b) single type particles-based nanocomposites after 48 h (c) hybrid type particles-based nanocomposites just after sonication, (d) hybrid particles-based nanocomposites after 48 h.

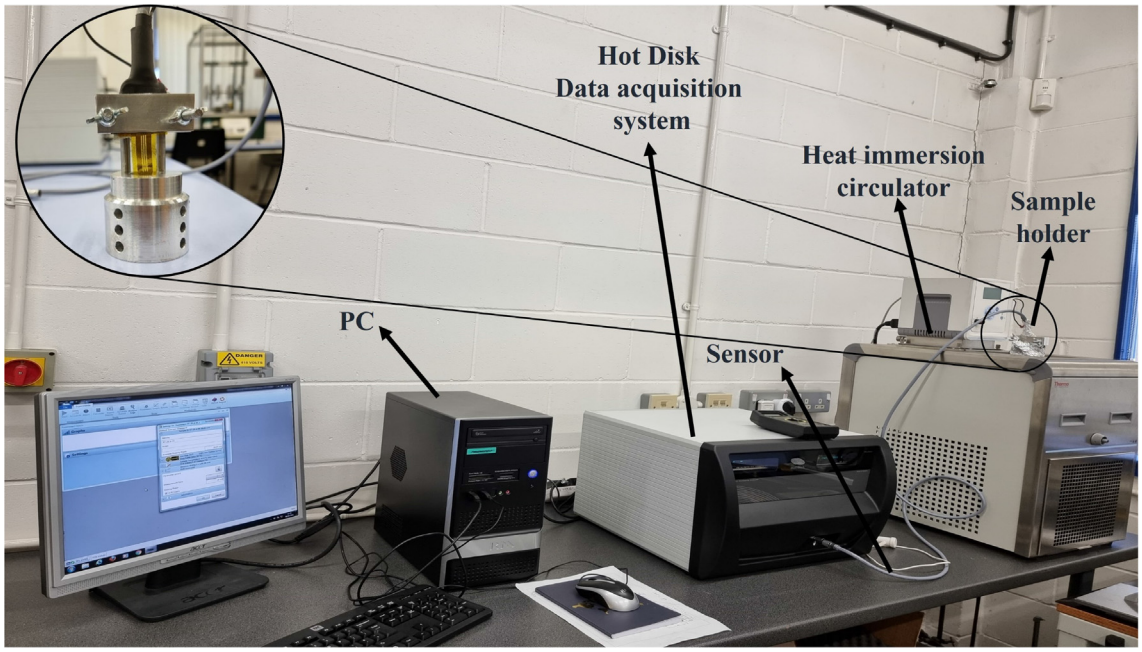

Fig. 4. Thermal conductivity testing setup with sample holder.

steel samples provided by the supplier, and the difference between the obtained experimental results and those provided in the manual was less than 0.5%, which is much less than the instrument measurement error (i.e., ± 5%).

3. Results and discussion

A thorough investigation was carried out to determine the influence of nanoparticles on the thermophysical properties of nano-PCMs. Thermal conductivity, FT-IR, XRD, DSC, and TGA are charac-

terisation methods that have been utilised to look into the characteristics of nano-enhanced phase change materials, and some interesting outcomes are reported.

3.1. Analysis of FT-IR spectra

FT-IR spectroscopy was used to investigate the chemical interactions and functional groups of base PCM, nanofillers, and composite PCMs impregnated with mono and hybrid nanofillers. For mono and hybrid nano-PCMs, samples with 1 wt% of nanoparticles were used to observe chemical interactions between the PCM and nanomaterials. FT-IR spectrum transmittance bands of GNP, MWCNTs, TiO_2, pure paraffin, PAR + GNP, PAR + MWCNTs, PAR + TiO_2, PAR/GNP + MWCNTs, PAR/GNP + TiO_2, PAR/MWCNTs + TiO_2 between the wavenumbers of 600 and 4000 cm^{-1} are shown in Fig. 5. No major stretching or bending peaks from MWCNTs and GNPs were observed in their infrared spectra since they lacked functional groups. The TiO_2 stretching vibrations are associated with the peaks at 635 and 643 cm^{-1}. Three transmittance peaks at 2945, 2905, and 2842 in the pristine paraffin spectrum showed moderate anti-symmetrical stretching vibrations of the $-CH_3$ and $-CH_2$- groups. In paraffin, the peak at 1490 indicated moderate C–H scissoring of the alkane (–CH2- and –CH3) groups. The modest rocking vibration of C–H in the long-chain methyl group can be seen in the peak at 750. Similar patterns of FT-IR spectra for nano-PCMs have been reported in different studies [39,40]. The FT-IR spectra of PAR + GNP, PAR + MWCNTs, PAR + TiO_2, PAR/GNP + MWCNTs, PAR/GNP + TiO_2, and PAR/MWCNTs + TiO_2 showed no substantial new peaks or significant peak shifts in the nano-PCMs, confirming that paraffin, GNP, MWCNTs, and SDBS only have physical interactions between them, and it is suggested that there is no chemical interaction between the PCM and nanoparticles.

3.2. XRD analysis

The crystallinity and unit cell dimensions of nanoparticles, paraffin, and paraffin embedded with single and hybrid particles were investigated utilising XRD. The XRD peaks obtained for the MWCNTs, GNP, TiO_2, paraffin, PAR/MWCNTs, PAR/GNP, PAR/TiO_2, PAR/MWCNTs + GNP, PAR/MWCNTs + TiO_2, and PAR/GNP + TiO_2 are shown in Fig. 6. For both the mono and hybrid nano-PCMs, the samples with 1.0 wt% of nanoparticles were used to see the crystal planes of the nano-PCMs. The diffraction peaks at 25.40° (002) and 42.50° (100) with PDF No. 00–058-1638 indicate the presence of MWCNTs [41]. The primary peaks in the XRD curve of GNP at 25.9°,42.0° and 45.3° may belong to the (002), (100) and (004) crystal planes of carbon from the GNP, correspondingly. The TiO_2 nanoparticle peaks at $2\theta = 25°$, 37.4°, 47.3°, and 53.8° correspond to the (101), (004), (200), respectively, and (105) lattice planes, confirming the anatase form of TiO_2 nanofillers with PDF No. 03–065-5714. The XRD sharp spectrum peaks of paraffin were obtained at 7.92°, 11.7°, 15.5°, 19.4°, 19.8°, 22.19°, 23.4°, 24.64°, 27.1°, 31.0°, 34.08°, 39.4°, and 44.3° with Miller indices (002), (003), (004), (010), (011), (401), (102), (111), (007), (008), (009), (122), and (0010), assigned to the crystal structure of n-octadecane identified in the crystallography open database. As the presence of nanofillers in a PCM is a small amount, fewer physical changes were observed. Because of the anatase crystal structure of TiO_2, the paraffin + TiO_2 composite has shown sharp intensities compared with the other nano-enhanced PCMs. Despite the high intensity of the paraffin + TiO_2 composite, no new peaks were identified, indicating that the pristine paraffin crystal structure was not altered by the addition of TiO_2 nanofillers. Hence, it is suggested that the paraffin crystal structure has not been changed, and the single and hybrid nano-PCMs hold the MWCNTs, GNP and TiO_2 peaks.

3.3. Phase-transition properties

Phase transition temperature and enthalpies of the pristine PCM and nano-PCMs with single and hybrid nanofillers during melting and solidification were examined using DSC. Fig. 7 (a - f) depict the melting and crystallisation processes of single and hybrid nanomaterial based PCMs at five different concentrations. The values of phase transition temperatures, enthalpies, and super-

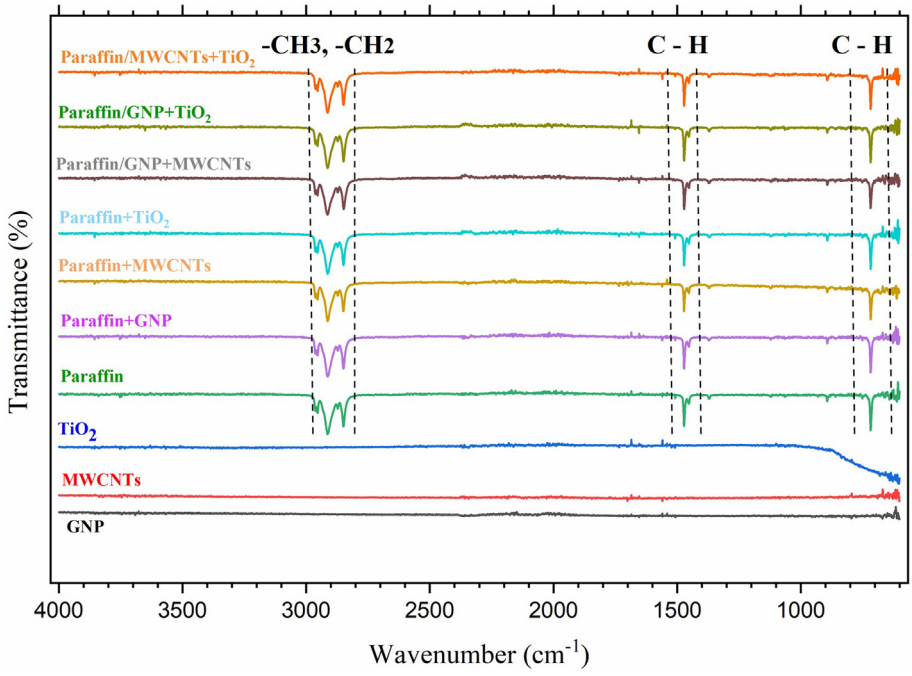

Fig. 5. FT-IR spectra of different samples.

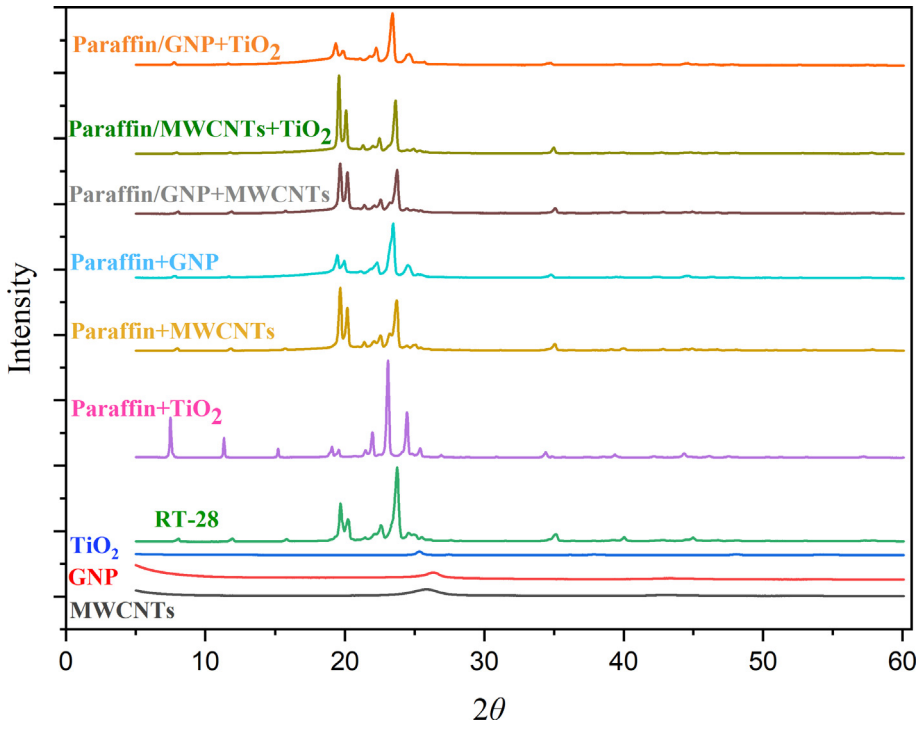

Fig. 6. XRD patterns of distinct single and hybrid nano-PCMs.

cooling degrees for both mono and hybrid nano-enhanced PCMs are listed in Tables 2 and 3, respectively. It can be seen that the incorporation of single and hybrid nanomaterials results in a very minor effect on the melting and solidification temperatures of the PCM. Similarly, a slight reduction in latent heat was observed with the inclusion of nano additives. During melting, a single endothermic peak is noticed for both pure paraffin and composites, which indicates isomorphous crystalline structures of both pure paraffin and paraffin composites. On the other hand, two exothermic peaks were identified in all samples during the solidification process. This bimodal crystallisation phenomenon refers to the metastable rotator phase that occurs before final crystallisation because of heterogeneous nucleation [42,43].

The supercooling degrees (ΔT) of single and hybrid nano-enhanced PCMs are reported in Tables 2 and 3, respectively. It can be seen that the degree of supercooling of the PCM was reduced after the incorporation of nanofillers. However, slight variations in TiO_2 based nano-PCMs are observed, which are attributed to the crystallisation confinement of titanium dioxide particles within the paraffin [39]. Overall, the decrease in Δ T demonstrates the increased importance of nanoparticles as nucleating agents in terms of effective homogenous nucleation and surface adsorption.

The latent heat of melting (ΔHm) and solidification (ΔHs) for the pristine paraffin were found to be 248.4 J/g and 251.7 J/g, correspondingly. It was observed that with an increase in the concentration of nanoparticles, the latent heat slightly decreased and the maximum reductions of −3.7%, −6.8%, −6.4%, −5.07%, −5.5%, and −5.2% and −4.12%, −7.31%, −7.2%, −6.9%, −6.4%, and −5.9% were seen at the highest concentration (i.e., 1.0 wt% of nanomaterials) for PAR + TiO_2, PAR + MWCNTS, PAR + GNP, PAR/MWCNTs + GNP, PAR/MWCNTs + TiO_2 and PAR/GNP + TiO_2 during melting and solidification, respectively. The reduction in latent heat could be due to the non-melting enthalpies of the nanofillers. In addition, single and hybrid titanium oxide particle based PCMs showed a smaller reduction in the latent heat of melting and crystallisation compared to carbon-based nano-PCMs. It has been reported [37] that the incorporation of TiO_2 nanofillers into the PCMs gives a negligible reduction in the latent heat. In some studies, an increase in the enthalpies was observed with the addition of TiO_2 nanomaterials, which could be due to the better stability and interactions between the TiO_2 particles and PCM molecules [37,44]. Conversely, the high thermal conductive carbon-based particles (i.e., MWCNTs, and GNP) have stability issues and due to their high thermal conductivities, as they accelerate the evaporation of paraffin, which affects the heat storage capability [8,32]. The theoretical value of the latent heat was also determined for all composites using Eq. (1) [45].

$$\Delta H_{nanoPCM} = \Delta H_{PCM}(1 - wt.\%) \quad (1)$$

where $\Delta H_{nanoPCM}$ signified the latent heat of nano-enhanced PCMs, ΔH_{PCM} signifies the latent heat of pristine paraffin, $wt.\%$ corresponds to the mass percentage of nanomaterials.

It is evident that the calculated latent heat of each PCM composite is greater than the latent heat measured in the laboratory with DSC. This could be due to the dispersion stability, surface morphology, and structure of the nanomaterials in the base PCM [46]. Overall, for all the PCM composites, no significant reduction in latent heat was observed; therefore, they may be used for thermal storage applications. Especially, TiO_2 based novel hybrid particle (MWCNTs + TiO_2 and GNP + TiO_2) based PCMs have the potential to be employed in buildings as energy storage materials since they have better stability, are economical, and have minimum effect on phase change enthalpies compared to carbon-based single and hybrid nanocomposites.

Fig. 8 shows how the specific heat capacity (the amount of heat needed to raise the temperature of a substance by a certain amount) of paraffin and nano-PCMs changes as the temperature increases from 10 °C to 55 °C in both solid and liquid states. The specific heat capacity has a relatively minimal effect on the overall amount of thermal energy that can be stored using these materials because of the low thermal energy density in the sensible heat storage phase. However, the specific heat capacity still affects other

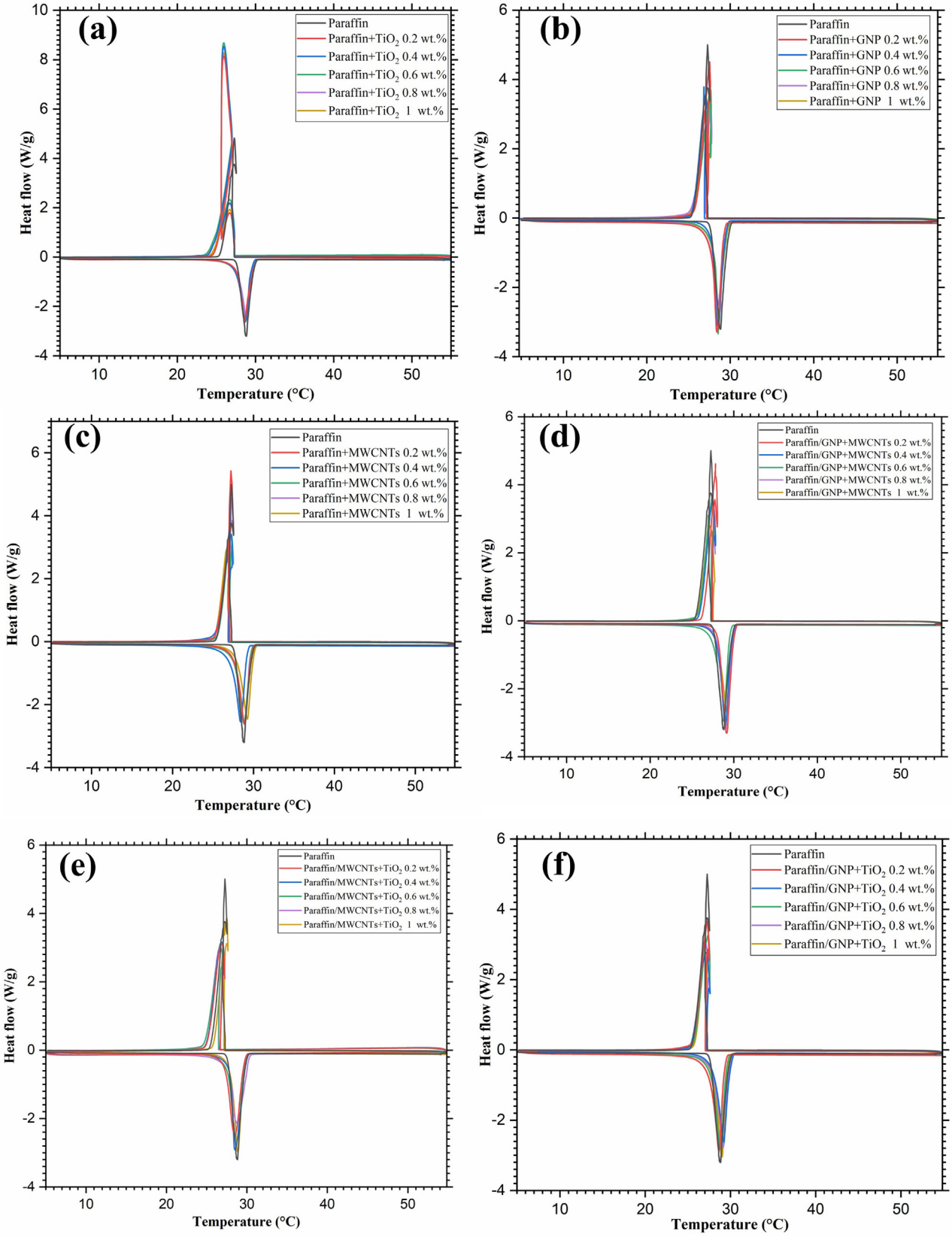

Fig. 7. A comparison of DSC results from single and hybrid nano enhanced PCMs (a) PAR + TiO_2, (b) PAR + GNP, (c) PAR + MWCNTs, (d) PAR/MWCNTs + GNP, (e) PAR/MWCNTs + TiO_2, and (f) PAR/GNP + TiO_2.

factors that affect the total amount of heat that can be stored within a certain temperature range by using these materials [47].

As shown in Fig. 8(a), the specific heat capacity of the nano-PCMs increased gradually as the temperature increased from

Table 2
Thermal properties of PCM composites with a single type of nanoparticles.

Sample	Melting				Crystallisation				
	T_{peak}	ΔHm_{exp}	ΔHm_{cal}	Relative error %	T_{peak}	ΔHm_{exp}	ΔHm_{cal}	Relative error %	ΔT
Paraffin (PAR)	28.92	248.4			27.26	251.7			1.66
PAR + TiO_2 0.2 wt%	28.67	247.1	247.90	0.32	26.46	249.3	251.19	0.75	2.21
PAR + TiO_2 0.4 wt%	28.68	246.7	247.40	0.28	26.32	247.2	250.69	1.39	2.36
PAR + TiO_2 0.6 wt%	28.79	244.1	246.90	1.13	26.54	246.02	250.18	1.66	2.25
PAR + TiO_2 0.8 wt%	28.84	243.8	246.41	1.06	26.86	244.73	249.68	1.98	1.98
PAR + TiO_2 1 wt%	28.83	239.2	245.4	2.52	26.67	241.32	249.18	3.15	2.16
PAR + MWCNTS 0.2 wt%	28.88	244.1	247.90	1.53	27.2	246.2	251.19	1.98	1.68
PAR + MWCNTS 0.4 wt%	28.4	239.7	247.40	3.11	27.24	241.1	250.69	3.82	1.16
PAR + MWCNTS 0.6 wt%	28.78	237.2	246.90	3.93	27.23	239.4	250.18	4.31	1.55
PAR + MWCNTS 0.8 wt%	28.8	235.5	246.41	4.42	27.08	236.7	249.68	5.20	1.72
PAR + MWCNTS 1 wt%	28.96	231.3	245.4	5.74	27.35	233.3	249.18	6.37	1.61
PAR + GNP 0.2 wt%	28.37	244.7	247.90	1.29	27.52	246.8	251.19	1.75	0.85
PAR + GNP 0.4 wt%	28.91	240.3	247.40	2.87	27.29	243.5	250.69	2.86	1.62
PAR + GNP 0.6 wt%	28.53	238.2	246.90	3.52	27.6	240.2	250.18	3.99	0.93
PAR + GNP 0.8 wt%	28.43	236.7	246.41	3.941678	27.64	238.6	249.68	4.03	0.79
PAR + GNP 1 wt%	28.59	232.4	245.4	5.29	27.67	233.5	249.18	4.96	0.92

T_{peak}: peak temperature (°C), **ΔHm_{exp}**: latent heat of melting experimental (J/g), **ΔHm_{cal}**: latent–heat of melting calculated (J/g), **RE**: relative error, **ΔT**: super–cooling degree (°C).

Table 3
Thermal properties of PCMs composites with hybrid types of nanoparticles.

Sample	Melting				Crystallisation				
	T_{peak}	ΔHm_{exp}	ΔHm_{cal}	Relative error %	T_{peak}	ΔHm_{exp}	ΔHm_{cal}	Relative error %	ΔT
Paraffin (PAR)	28.92	248.4			27.26	251.7			1.66
PAR/MWCNTs + GNP 0.2 wt%	28.95	242.8	247.90	2.05	27.82	245.1	251.19	2.42	1.13
PAR/MWCNTs + GNP 0.4 wt%	28.89	239.6	247.40	3.15	27.41	241.5	250.69	3.66	1.48
PAR/MWCNTs + GNP 0.6 wt%	28.71	237.76	246.90	3.70	27.46	239.3	250.18	4.35	1.25
PAR/MWCNTs + GNP 0.8 wt%	28.94	235.8	246.41	4.30	27.42	236.2	249.68	5.40	1.52
PAR/MWCNTs + GNP 1 wt%	28.96	230.9	245.4	5.90	27.19	234.1	249.18	6.05	1.77
PAR/MWCNTs + TiO_2 0.2 wt%	28.49	245.7	247.90	0.88	26.84	247.5	251.19	1.47	1.65
PAR/MWCNTs + TiO_2 0.4 wt%	28.5	243.3	247.40	1.65	26.85	245.7	250.69	1.99	1.65
PAR/MWCNTs + TiO_2 0.6 wt%	28.53	239.5	246.90	3.00	26.72	241.8	250.18	3.35	1.81
PAR/MWCNTs + TiO_2 0.8 wt%	28.78	236.5	246.41	4.02	26.69	239.7	249.68	3.99	2.09
PAR/MWCNTs + TiO_2 1 wt%	28.86	234.6	245.4	4.40	27.48	235.5	249.18	5.49	1.38
PAR/GNP + TiO_2 0.2 wt%	28.62	246.5	247.90	0.56	27.26	248.1	251.19	1.23	1.36
PAR/GNP + TiO_2 0.4 wt%	28.98	243.8	247.40	1.45	27.16	246.3	250.69	1.75	1.82
PAR/GNP + TiO_2 0.6 wt%	28.78	240.2	246.90	2.71	27.36	241.9	250.18	3.31	1.42
PAR/GNP + TiO_2 0.8 wt%	28.93	237.1	246.41	3.77	27.09	240.2	249.68	3.79	1.84
PAR/GNP + TiO_2 1 wt%	28.88	235.4	245.4	4.07	27.2	236.8	249.183	4.68	1.68

T_{peak}: peak temperature (°C), **ΔHm_{exp}**: latent heat of melting experimental (J/g), **ΔHm_{cal}**: latent–heat of melting calculated (J/g), **RE**: relative error, **ΔT**: super–cooling degree (°C).

10 °C to 25 °C in the solid phase. In contrast, the specific heat capacity remained constant in the liquid phase, as shown in Fig. 8(b). The results of the specific heat capacity analysis for both phases demonstrated concurrence with prior research findings [48–50]. The specific heat capacity of paraffin was 1.928 J/g °C in the solid phase and 1.887 J/g °C in the liquid phase. It is evident that the addition of nanoparticles to the PCMs increased the specific heat capacity in both the solid and liquid phases. At 25 °C and 55 °C, the specific heat capacities of the nano-PCMs were 4.011 J/g °C and 2.556 J/g °C, respectively.

3.4. Thermal reliability

The thermal stability of PCM and composites was examined using TGA and DTG (derivative thermogravimetric analysis). The TGA curves of the pristine and nano-PCMs are displayed in Fig. 9 (a – f). It can be seen from the TGA peaks that there is no discernable mass loss up to ~ 130 °C for either paraffin or its composites. As the temperature increased, the weight loss became more pronounced, reaching its maximum degradation temperature while leaving a constant residue behind. For pure paraffin, the maximum degradation temperature observed was 211.34 °C with 0.8272% residue. The evaporation of paraffin causes such decomposition, wherein hydrocarbon chains disintegrate into monomers. Furthermore, it was discovered that with the inclusion of nanoparticles, the maximum degradation temperature increased because highly thermally conductive nanoparticles improved the thermal conductivity of the nano-PCMs, which resulted in faster and more uniform heat transfer. With an increase in the weight percentage of nanoparticles, the final, residual, initial, and onset temperatures increased. Basically, the nanomaterials form a shielding layer on the surface of paraffin which impedes vaporisation during thermal deprivation. The DTG peaks of the samples shown in Fig. 10 (a – f) demonstrate that all the mono and hybrid nano-PCMs have similar thermal decompositions. As no weight loss was observed until ~ 130 °C for all samples, therefore the developed nano-PCMs have the potential to be employed in buildings and other thermal energy storage applications.

3.5. Thermal conductivity

The major purpose of PCMs is to properly capture and discharge thermal energy during melting and solidification. Thermal conductivity determines how fast the thermal energy is stored and

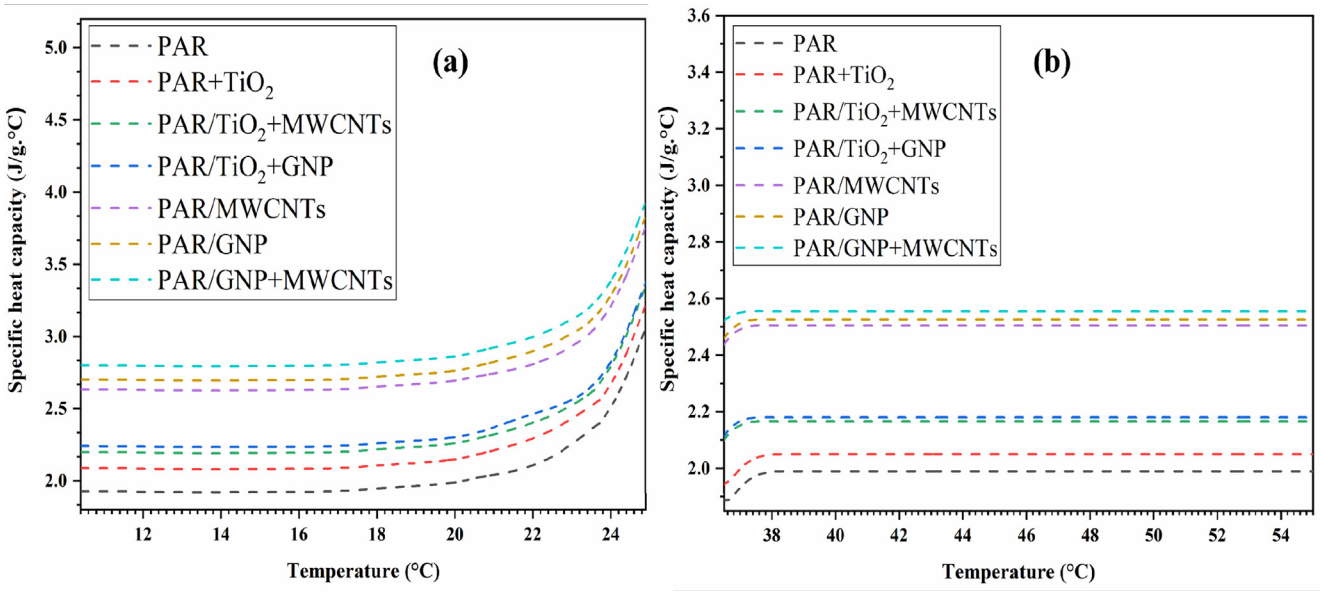

Fig. 8. Specific heat capacity of paraffin and nano-PCMs versus temperature (a) in a solid phase and (b) in a liquid phase.

released during the melting and crystallisation of the PCM. Pure PCMs have poor thermal conductivity, which limits the rate of heat storage and release and restricts their applications. A PCM with greater thermal conductivity decreases the melting and solidification time and accelerates the heat transfer during these processes [25]. Thermal conductivity of the pure PCM, single, and hybrid PCM samples (PAR + GNP, PAR + MWCNTs, PAR + TiO_2, PAR/GNP + MWCNTs, PAR/GNP + TiO_2, and PAR/MWCNTs + TiO_2) were measured at six different temperatures ranging from 5 °C to 25 °C for solids and 30 °C to 55 °C for liquids, as illustrated in Fig. 11 (a – f).

As shown in Fig. 11 (a) and (b), at 5 °C and 15 °C, nano-PCMs were solid, and as the nanoparticle loading concentration increased, MWCNTs and GNP-based mono and hybrid nanoparticle based PCMs demonstrated higher thermal conductivity than TiO_2 and TiO_2-based hybrid particle based PCMs. It can be seen that the mono and hybrid carbon-based nano-PCMs have shown greater enhancement because of the superior thermal conductivities of GNP and MWCNTs nanofillers. Overall, GNP + MWCNTs hybrid nanoparticles-based nano-PCMs showed higher thermal conductivity in comparison to TiO_2 + MWCNTs and TiO_2 + GNP since they have a higher concentration (70 wt%) of TiO_2 and lower concentration of GNP and MWCNTs (30 wt%). Therefore, due to lower thermal conductivity, titanium oxide TiO_2 + MWCNTs and TiO_2 + GNP type hybrid nano-PCMs have shown lower conductivity but they performed better than mono TiO_2 nanoparticles based PCM.

Similar thermal conductivity trends were observed at 25 °C but a significant increase in the thermal conductivity was detected at 25 °C as can be seen in Fig. 11 (c). As the melting temperature of the PCM is 28 °C, and near melting temperature nano-PCMs are in a metastable state, the crystalline arrangement of the PCM becomes unstable and a surge in temperature quickens the molecular vibration in the lattice, therefore the thermal conductivity of pristine PCM and nano-PCMs rises abruptly near the melting temperature (i.e., 25 °C) [51]. The thermal conductivities of 0.29, 0.82, 0.61, 0.4, 0.864, 0.51 and 0.484 W/m.k were obtained for paraffin, PAR + GNP, PAR + MWCNTs, PAR + TiO_2, PAR/GNP + MWCNTs, PAR/GNP + TiO_2, and PAR/MWCNTs + TiO_2 at 1 wt%, respectively.

In the liquid phase at 35 °C, 45 °C and 55 °C, the thermal conductivity values obtained for mono and hybrid nano-PCMs were below 0.2 W/m.K. Although as in the solid state a constant trend was observed in the liquid state, in that the thermal conductivity decreased significantly as shown in Fig. 11 (d–f). The cause for exceptionally low TC at 35 °C, 45 °C, and 55 °C is that at these temperatures, the PCM is completely melted, and the arranged microstructure of the PCM in the solid state has been changed to a disorganised microstructure in the liquid state. In addition, heat is conducted by lattice vibrations in solids as molecules move within their lattice structures. Solids are more effective than liquids in terms of their lattice vibration and free-electron motion. Thus, solid PCMs have a greater thermal conductivity value than those of the liquid PCMs.

The percentage enhancement in the thermal conductivities after the dispersion of nanofillers was also measured at temperatures ranging from 5 °C to 55 °C, as shown in Fig. 12 (a – f). The thermal conductivity enhancement factor was calculated using equation (2):

$$\eta = \frac{K_{nano-PCM} - K_{PCM}}{K_{PCM}} * 100 \quad (2)$$

where $K_{nano-PCM}$ and K_{PCM} are the thermal conductivities of nano-enhanced PCMs and pristine PCM, respectively.

As demonstrated in Fig. 12 (a) and (b), the carbon-based (GNP + MWCNTs) hybrid nanofillers attained higher enhancements in effective thermal conductivities with maximum enhancements of 101.53% and 97.98% observed at 1 wt% of PAR/GNP + MWCNTs at temperatures of 5 °C and 15 °C, respectively. On the other hand, TiO_2 based nano-PCM depicted the lowest enhancement because of its low thermal conductivity. In addition, with an increase in the percentage concentration of the nanoparticles, the thermal conductivity enhancement increased.

The significant relative enhancement in the thermal conductivity with carbon-based nanoparticles can be seen in Fig. 12(c). The hybrid nanoparticles showed substantial improvements of 170%, 75.8%, and 66.89% for GNP/MWCNTs, GNP + TiO_2, and MWCNTs + TiO_2 at 1 wt%, respectively. As mentioned earlier, the large improvement of PCM composites in the thermal conductivity at 25 °C is because vibrations within the molecule lattice structures of the PCM and PCM composites increase near the melting temperature (i.e., 28 °C), which results in a sudden increase in thermal conductivity of nano-PCMs.

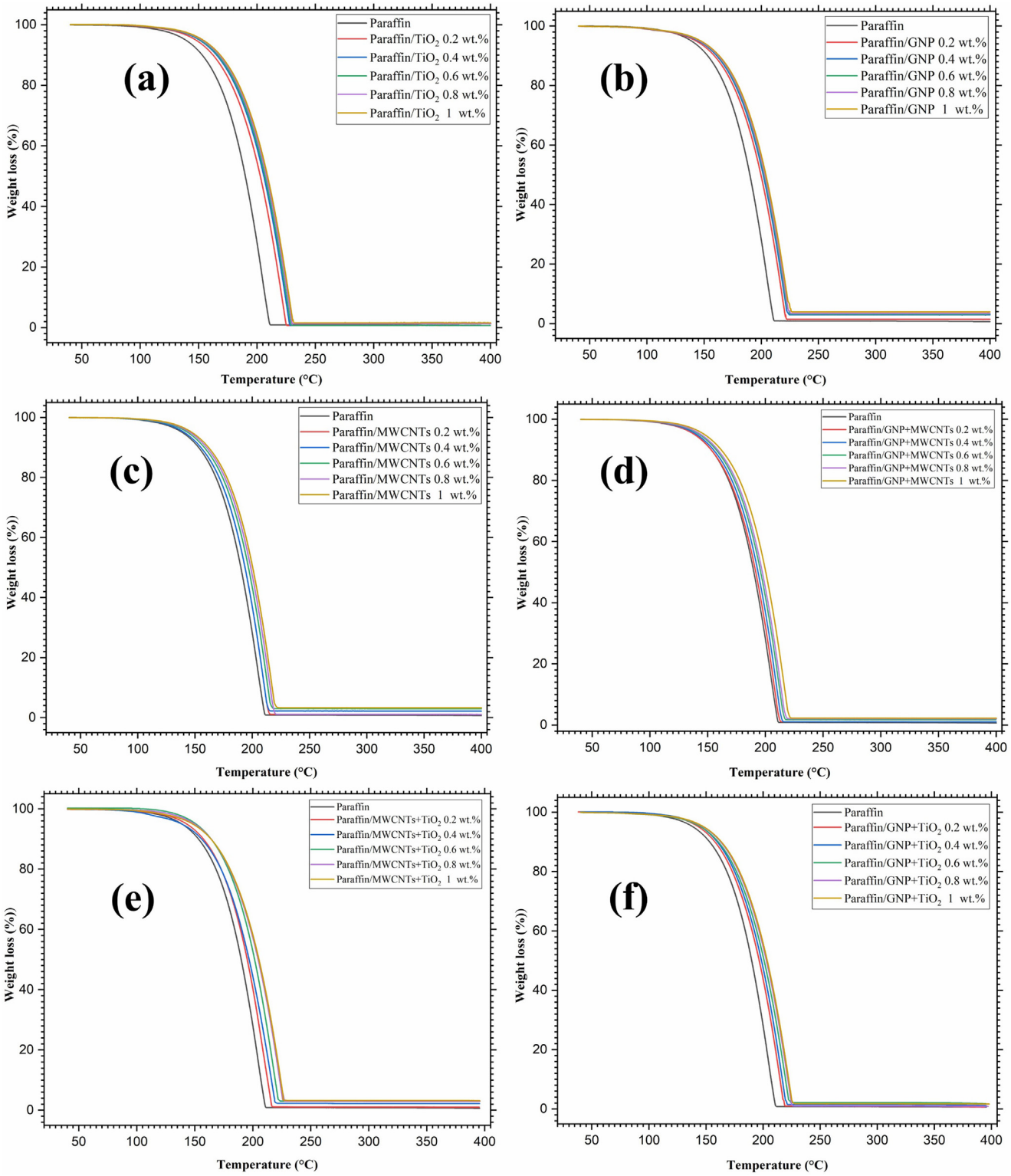

Fig. 9. TGA curves of single and hybrid nano enhanced PCMs (a) PAR + TiO_2, (b) PAR + GNP, (c) PAR + MWCNTs, (d) PAR/MWCNTs + GNP, (e) PAR/MWCNTs + TiO_2, and (f) PAR/GNP + TiO_2.

However, when nano-PCMs were changed to complete liquid form at 35 °C, 45 °C and 55 °C, the comparative enhancement in thermal conductivity was lower than with solids. As illustrated in Fig. 12 (d-f), the maximum enhancement in thermal conductivity was no more than 45% for all the PCM composites. As with solids, GNP + MWCNTs based PCM showed maximum enhancement compared to the other nano-PCMs at 35 °C, 45 °C and 55 °C.

Overall, TC results have shown that with the addition of the particles, the thermal conductivities of single and hybrid nano-PCMs were increased because the employed nanomaterials have greater thermal conductivities in comparison to the base PCM. In addition,

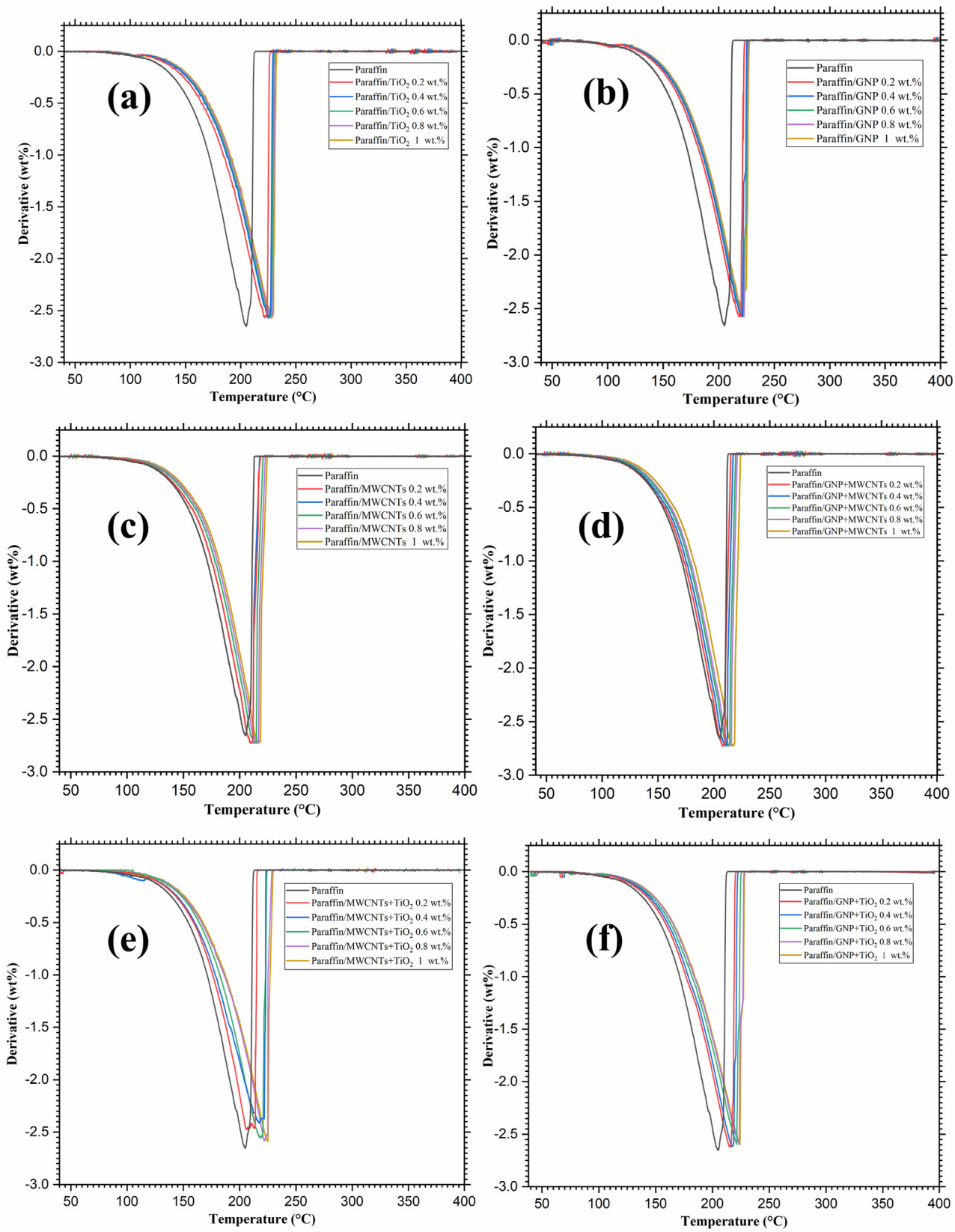

Fig. 10. DTG curves of single and hybrid nano enhanced PCMs (a) PAR + TiO_2, (b) PAR + GNP, (c) PAR + MWCNTs, (d) PAR/MWCNTs + GNP, (e) PAR/MWCNTs + TiO_2, and (f) PAR/GNP + TiO_2.

higher values of thermal conductivities were observed in the temperature range of 5 °C to 25 °C, when the PCM is in solid form. In contrast, the thermal conductivity values significantly decreased at higher temperatures (35 °C to 55 °C) when the PCM was in liquid

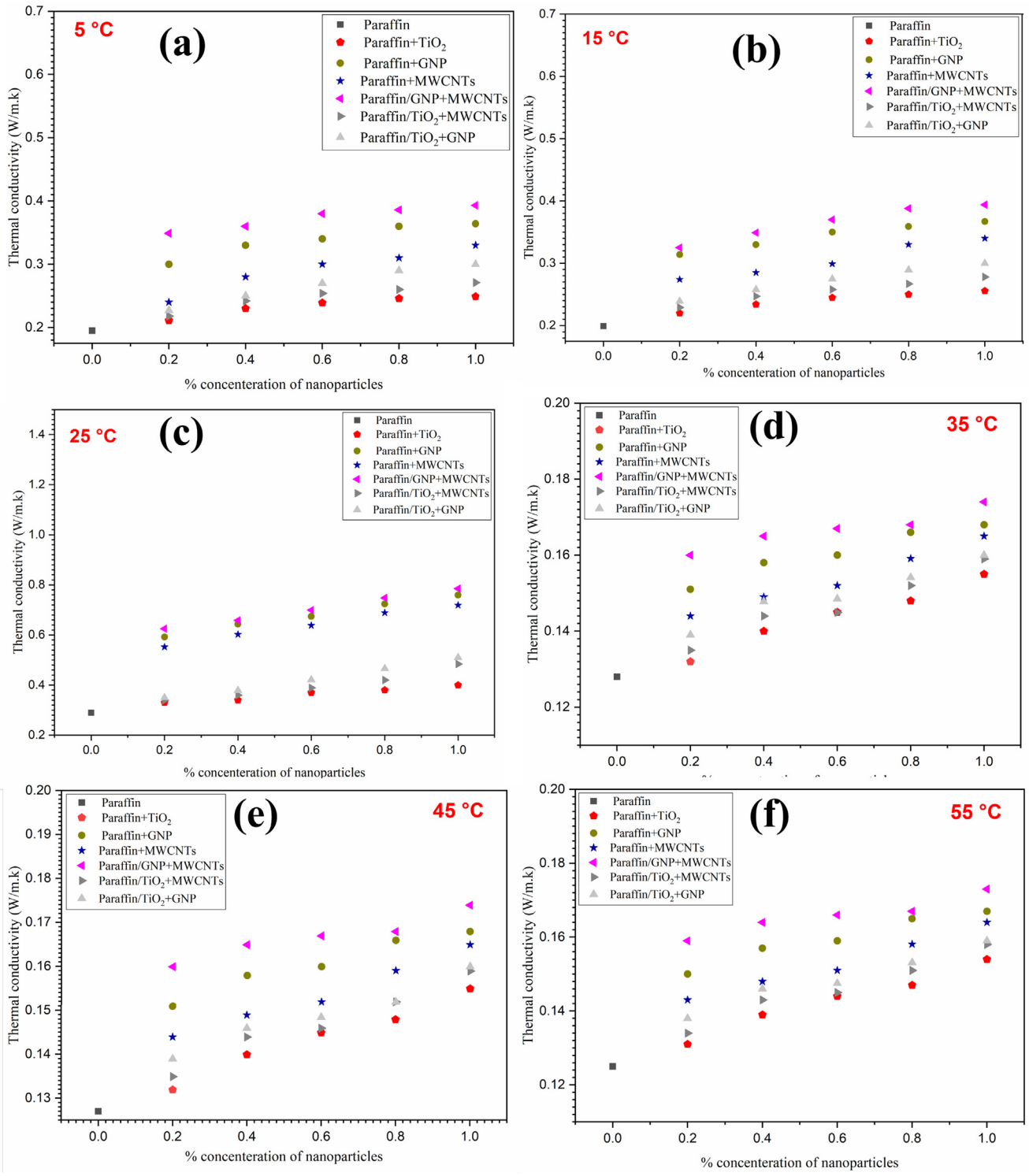

Fig. 11. Influence of nanofillers concentration on thermal conductivity at various temperatures.

form. This shows that the temperature influenced on the thermal conductivity of PCMs. In comparison to the other nano-PCMs, it can be suggested that the GNP + MWCNTs based PCM demonstrated the greatest improvement at all temperatures. This is because carbon-based nano additives are known to have superior physical properties such as hydrogen bonding, capillarity, and surface tension, which enable the adsorption of fresh samples on their pores and surfaces during phase transition without leakage [52].

3.6. Repeatability

The repeatability of experimental work is critical, especially in the case of nanofluids, such as liquid nano-PCMs. The characteristics repeatability of the nanofluids ensured their stability during a period of time. Therefore, after 48 h, the thermal conductivity of prepared mono and hybrid nano-PCMs were tested; the results are presented in Fig. 13. It can be seen that good repeatability has been achieved. As shown in Fig. 13, a maximum deviation

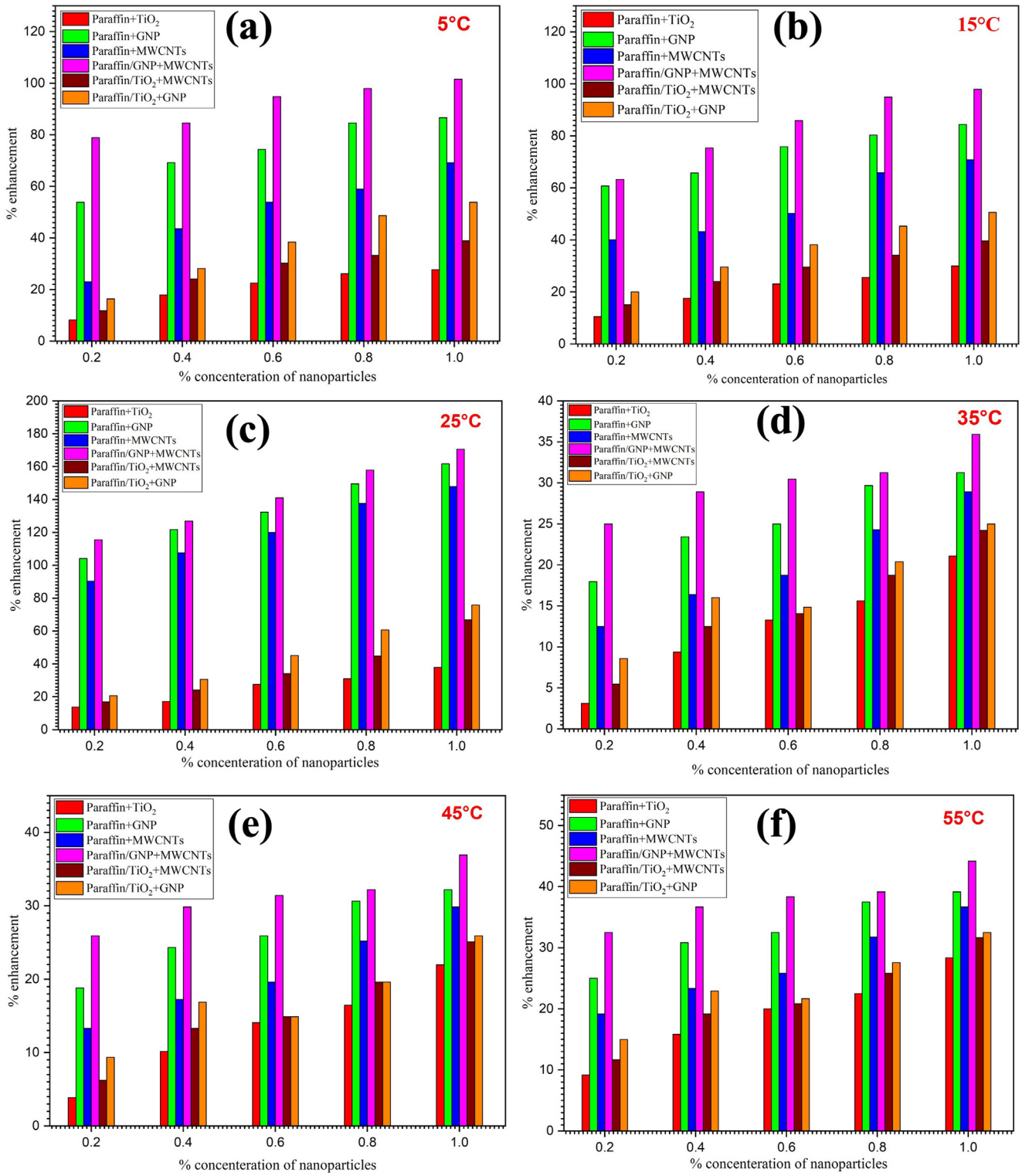

Fig. 12. Impact of particles concentration on TC enhancement at different temperatures.

of ± 5% was observed for hybrid nano-PCMs, and ± 8 % for single nano-PCMs excluding MWCNTs based nano-PCMs. The thermal conductivity of single type MWCNTs decreased significantly after 48 h, potentially due to their hydrophobic nature, and the MWCNTs settled down after 48 h, as shown in Fig. 13 (a). However, all other single and hybrid nano-PCMs were found to be very stable. The thermal stability of the phase change material (PCM) and the nanoparticle-modified PCMs (nano-PCMs) was also evaluated by subjecting them to 100 heating and cooling cycles. As shown in Fig. 14, the phase-change properties of the materials were not significantly affected by the thermal cycles since there are no additional secondary curves in the differential scanning calorimetry (DSC) graphs. The variations in the phase change temperatures and enthalpies for the nano-PCMs were less than 1%, indicating a promising level of stability to be employed in an application. The thermal stability above 100 thermal cycles was also

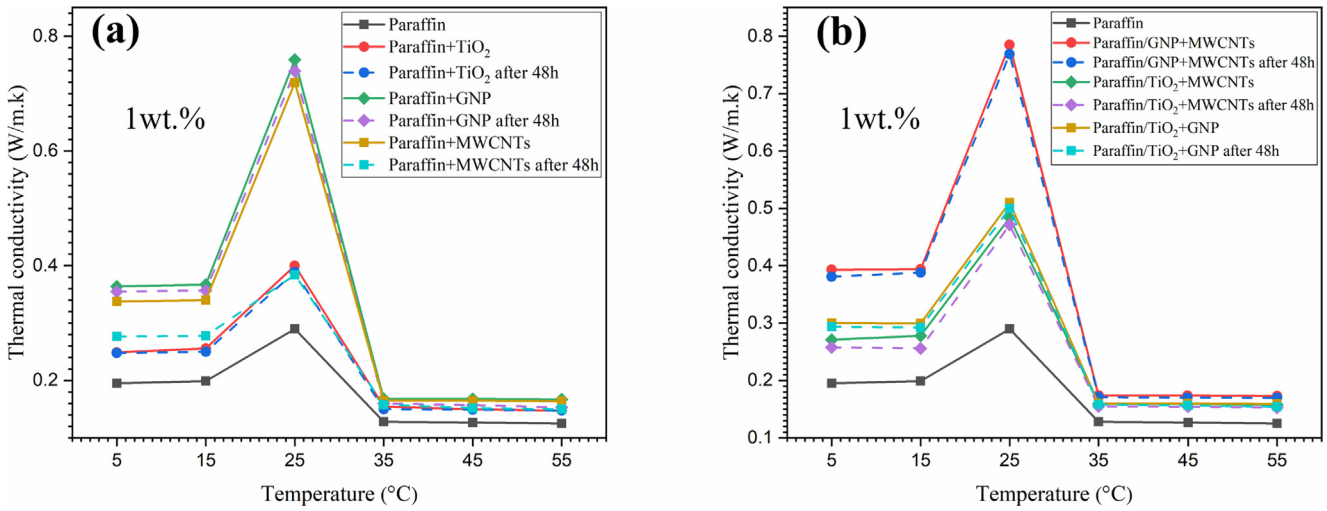

Fig. 13. Thermal conductivities versus temperature of nano phase PCMs after 48 h (a) single, and (b) hybrid nano-enhanced phase change materials for thermal conductivity after 48 h.

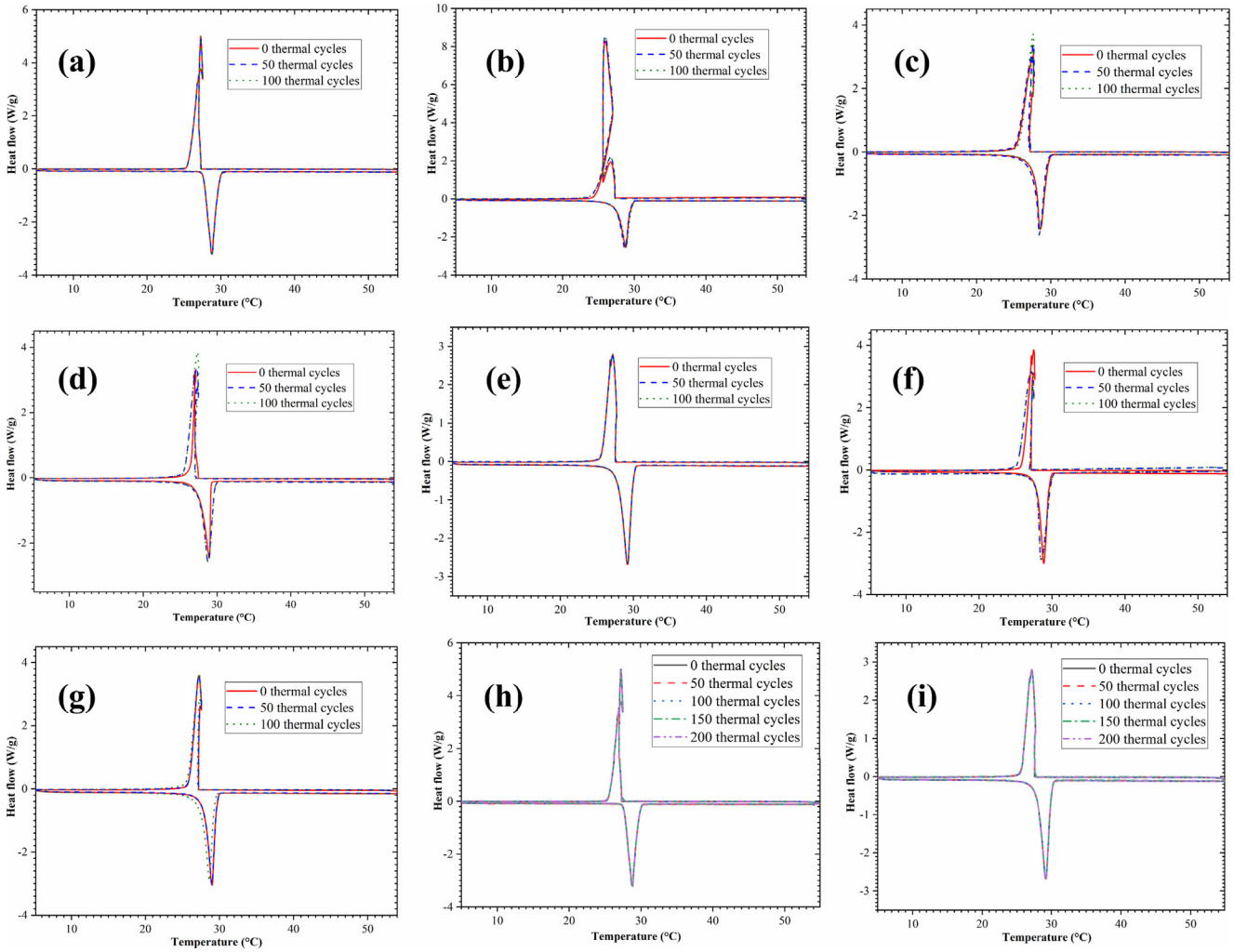

Fig. 14. DSC thermal cycle curves of single and hybrid nano enhanced PCMs (a, h) PAR (b) PAR + TiO_2, (c) PAR + GNP, (d) PAR + MWCNTs, (e, i) PAR/MWCNTs + GNP, (f) PAR/MWCNTs + TiO_2, and (g) PAR/GNP + TiO_2.

tested where two samples of pure paraffin and paraffin enhanced hybrid nanoparticle based PCM (i.e., GNP + MWCNTs), were subjected to 200 cycles of heating and cooling. As shown in Fig. 14 (h and i), both samples were found to have remained stable after

200 thermal cycles without experiencing any notable changes, demonstrating the high stability of both pure PCM and nano-enhanced PCMs. This suggests their capability to be used in thermal energy storage applications.

To investigate the chemical interactions of the samples after 100 thermal cycles, FTIR analysis was performed. For both the mono-and hybrid nano-PCMs, the samples with 1 wt% of nanoparticles were used to observe chemical interactions between the PCM and nanomaterials. As shown in Fig. 15, the FT-IR spectra of the samples treated 100 times (i.e., PAR, PAR + GNP, PAR + MWCNTs, PAR + TiO2, PAR/GNP + MWCNTs, PAR/GNP + TiO2, and PAR/MWCNTs + TiO2) showed no substantial new peaks or significant peak shifts in the nano-PCMs. This is to confirm that paraffin, GNP, TiO2, MWCNTs, and SDBS have only physical interactions between them, and they do not have any chemical interaction between the PCM and nanoparticles even after 100 thermal cycles.

4. Conclusions and future work

The present experimental investigation explored the thermophysical characteristics of GNP, MWCNTs, TiO_2 mono and hybrid nanoparticle based PCM nanocomposites. Different characterisation techniques which include DSC, TEM, FT-IR, TGA, XRD, and thermal conductivity equipment were employed to explore the ideal thermal properties for the efficient thermal energy storage materials. The key findings of the current investigation are given as follows.

- The results of FT-IR and XRD analysis demonstrate that the addition of GNP, MWCNTs, and TiO_2 as mono or hybrid particles to pristine paraffin results in only physical interactions, as indicated by the absence of new peaks in the FT-IR spectra. Furthermore, the XRD profiles indicate that the crystal structure of the paraffin remains unchanged after the addition of nanofillers. The absence of new peaks in the FT-IR and XRD profiles indicates that these nanoparticles are chemically compatible with paraffin.
- DSC analysis has revealed that the inclusion of nanoparticles has almost no effect on the peak melting and solidification of nano-PCMs. However, a slight reduction in latent heat has been observed, with a maximum reduction of −7 %, and −6.9 % observed for the latent heat of melting and crystallisation with the hybrid GNP + MWCNT based nano-PCM, respectively. Moreover, for the paraffin/TiO_2, a minimum decrease of −3.7 % and −4.1 % in the latent heat of fusion and solidification has been noticed.
- DTG and TGA curves illustrate that all unitary and hybrid nano-PCMs have shown good chemical and thermal stability. Also, the addition of nano additives enhanced the chemical and thermal stability of the nano-PCMs.
- The thermal conductivity results revealed that the GNP + MWCNTs based hybrid nano-PCM had maximum thermal conductivity at all temperatures. In addition, higher thermal conductivity was observed at 5 °C, 15 °C and 25 °C respectively when the PCM was in solid state and it decreased abruptly when it was changed into liquid state at 35 °C, 45 °C and 55 °C. The thermal conductivity of nano-PCMs increases linearly with concentration of particles, and the carbon-based particle nano-PCM performed better than the titanium oxide particle based nano-PCM.
- It is evident that the developed nano-enhanced PCMs demonstrated enhanced thermal properties. In particular, TiO_2 based novel hybrid particles (TiO_2 + MWCNTs and TiO_2 + GNP) based PCMs have the potential to be employed for thermal energy storage applications since the 70% of TiO_2 particles in these hybrid combinations make them stable and cost-effective, as TiO_2 nanoparticles have better stability and low cost compared to MWCNTs and GNP. Also, they exhibit overall better performance compared to single particle-based nano-PCMs.

In this study, single and hybrid nanoparticles were used unmodified; however, for future research, these particle surfaces could be modified to investigate the effect of surface modification on the thermophysical properties of nano-PCMs. Furthermore,

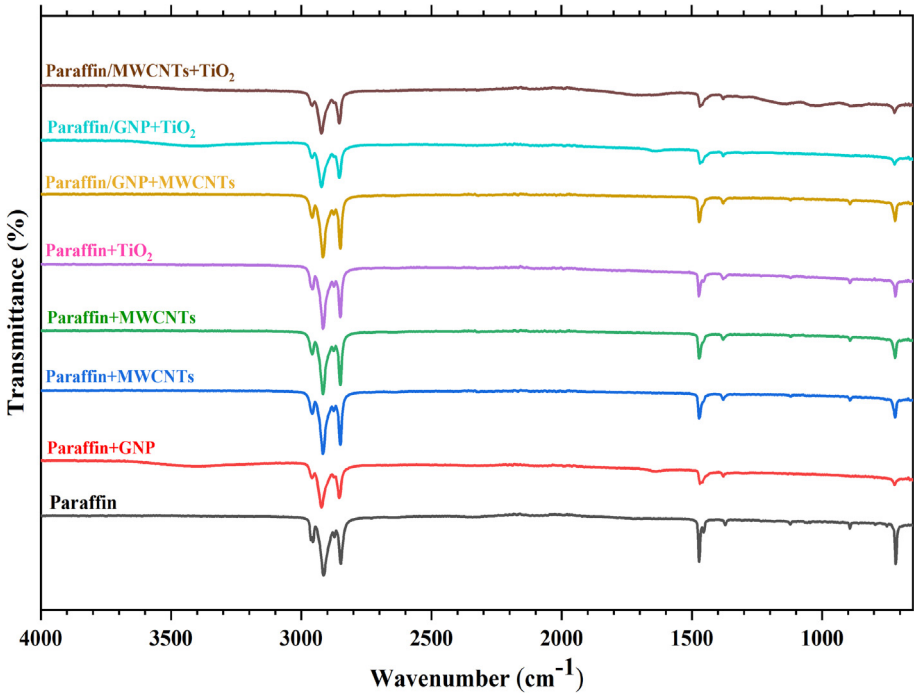

Fig. 15. FT-IR spectra of thermally treated samples.

there have been numerous studies on organic PCM-based nanocomposites; nevertheless, the use of inorganic PCMs should not be overlooked because they have excellent thermophysical properties and are particularly useful for high-temperature energy storage applications.

CRediT authorship contribution statement

Muhammad Aamer Hayat: Conceptualization, Writing – original draft. **Y Yang:** Supervision. **Liang Li:** Supervision. **Mose Bevilacqua:** Supervision. **Yong Kang Chen:** Supervision.

Data availability

Data will be made available on request.

Declaration of Competing Interest

The authors declare that they have no known competing financial interests or personal relationships that could have appeared to influence the work reported in this paper.

Acknowledgements

The authors would like to acknowledge financial support of the European Union's Horizon 2020 research and innovation programme under the Marie Skłodowska-Curie grant agreement No 801604 and the Royal Society (RGS\R2\222256 and IES\R3 \183069).

References

[1] Y. Li, Z. Ding, M. Shakerin, N. Zhang, A multi-objective optimal design method for thermal energy storage systems with PCM: A case study for outdoor swimming pool heating application, J Energy Storage. 29 (2020).
[2] G. Wei, G. Wang, C. Xu, X. Ju, L. Xing, X. Du, Y. Yang, Selection principles and thermophysical properties of high temperature phase change materials for thermal energy storage: a review, Renew. Sustain. Energy Rev. 81 (2018) 1771–1786.
[3] G. Alva, Y. Lin, G. Fang, An overview of thermal energy storage systems, Energy 144 (2018) 341–378.
[4] H.M. Ali, A. Saieed, W. Pao, M. Ali, Copper foam/PCMs based heat sinks: an experimental study for electronic cooling systems, Int. J. Heat Mass Transf. 127 (2018) 381–393.
[5] H. Usman, H.M. Ali, A. Arshad, M.J. Ashraf, S. Khushnood, M.M. Janjua, S.N. Kazi, An experimental study of PCM based finned and un-finned heat sinks for passive cooling of electronics, Heat Mass Transf. 54 (2018) 3587–3598.
[6] M.A. Hayat, H.M. Ali, M.M. Janjua, W. Pao, C. Li, M. Alizadeh, Phase change material/heat pipe and Copper foam-based heat sinks for thermal management of electronic systems, J Energy Storage. 32 (2020).
[7] S.L. Tariq, H.M. Ali, M.A. Akram, M.M. Janjua, Experimental investigation on graphene based nanoparticles enhanced phase change materials (GbNePCMs) for thermal management of electronic equipment, J Energy Storage. 30 (2020).
[8] A.S. Abdelrazik, F.A. Al-Sulaiman, R. Saidur, Numerical investigation of the effects of the nano-enhanced phase change materials on the thermal and electrical performance of hybrid PV/thermal systems, Energy Convers Manag. 205 (2020).
[9] N. Aslfattahi, R. Saidur, A. Arifutzzaman, R. Sadri, N. Bimbo, M.F.M. Sabri, P.A. Maughan, L. Bouscarrat, R.J. Dawson, S.M. Said, Experimental investigation of energy storage properties and thermal conductivity of a novel organic phase change material/MXene as A new class of nanocomposites, J Energy Storage. 27 (2020).
[10] J.M. Khodadadi, L. Fan, H. Babaei, Thermal conductivity enhancement of nanostructure-based colloidal suspensions utilized as phase change materials for thermal energy storage: a review, Renew. Sustain. Energy Rev. 24 (2013) 418–444.
[11] L.-W. Fan, X. Fang, X. Wang, Y. Zeng, Y.-Q. Xiao, Z.-T. Yu, X. Xu, Y.-C. Hu, K.-F. Cen, Effects of various carbon nanofillers on the thermal conductivity and energy storage properties of paraffin-based nanocomposite phase change materials, Appl. Energy 110 (2013) 163–172.
[12] A. Arshad, M. Jabbal, L. Shi, Y. Yan, Thermophysical characteristics and enhancement analysis of carbon-additives phase change mono and hybrid materials for thermal management of electronic devices, J Energy Storage. 34 (2021), https://doi.org/10.1016/j.est.2020.102231.
[13] P. Dixit, A. Konala, V.J. Reddy, J. Singh, A. Dasari, S. Chattopadhyay, Thermal performance evaluation of isopropyl stearate-expanded graphite based shape stabilized phase change material composite targeting cold chain application, J. Mol. Liq. 363 (2022).
[14] S. Harish, D. Orejon, Y. Takata, M. Kohno, Thermal conductivity enhancement of lauric acid phase change nanocomposite with graphene nanoplatelets, Appl. Therm. Eng. 80 (2015) 205–211.
[15] S. Harish, D. Orejon, Y. Takata, M. Kohno, Enhanced thermal conductivity of phase change nanocomposite in solid and liquid state with various carbon nano inclusions, Appl. Therm. Eng. 114 (2017) 1240–1246.
[16] G. Wang, Y. Yang, S. Wang, Thermophysical properties analysis of graphene-added phase change materials and evaluation of enhanced heat transfer effect in underwater thermal vehicles, J. Mol. Liq. 348 (2022).
[17] F. Bahiraei, A. Fartaj, G.-A. Nazri, Experimental and numerical investigation on the performance of carbon-based nanoenhanced phase change materials for thermal management applications, Energy Convers Manag. 153 (2017) 115–128.
[18] V. Chinnasamy, H. Cho, Investigation on thermal properties enhancement of lauryl alcohol with multi-walled carbon nanotubes as phase change material for thermal energy storage, Case Studies in Thermal Engineering. 31 (2022).
[19] T.-P. Teng, C.-M. Cheng, C.-P. Cheng, Performance assessment of heat storage by phase change materials containing MWCNTs and graphite, Appl. Therm. Eng. 50 (2013) 637–644.
[20] H. Babaei, P. Keblinski, J.M. Khodadadi, Thermal conductivity enhancement of paraffins by increasing the alignment of molecules through adding CNT/graphene, Int. J. Heat Mass Transf. 58 (2013) 209–216.
[21] Z.A. Nawsud, A. Altouni, H.S. Akhijahani, H. Kargarsharifabad, A comprehensive review on the use of nano-fluids and nano-PCM in parabolic trough solar collectors (PTC), Sustainable Energy Technol. Assess. 51 (2022).
[22] A. Stonehouse, C. Abeykoon, Thermal properties of phase change materials reinforced with multi-dimensional carbon nanomaterials, Int. J. Heat Mass Transf. 183 (2022).
[23] H. Xie, L. Chen, Review on the preparation and thermal performances of carbon nanotube contained nanofluids, J. Chem. Eng. Data 56 (2011) 1030–1041.
[24] W. Jiang, G. Ding, H. Peng, Measurement and model on thermal conductivities of carbon nanotube nanorefrigerants, Int. J. Therm. Sci. 48 (2009) 1108–1115.
[25] M.A. Hayat, Y. Chen, M. Bevilacqua, L. Li, Y. Yang, Characteristics and potential applications of nano-enhanced phase change materials: A critical review on recent developments, Sustainable Energy Technol. Assess. 50 (2022).
[26] E.J. D'Oliveira, S.C.C. Pereira, D. Groulx, U. Azimov, Thermophysical properties of Nano-enhanced phase change materials for domestic heating applications, J Energy Storage. 46 (2022).
[27] K.Y. Leong, M.R.A. Rahman, B.A. Gurunathan, Nano-enhanced phase change materials: A review of thermo-physical properties, applications and challenges, J Energy Storage. 21 (2019) 18–31.
[28] L. Yang, J. Huang, F. Zhou, Thermophysical properties and applications of nano-enhanced PCMs: An update review, Energy Convers Manag. 214 (2020).
[29] B.E. Jebasingh, A.V. Arasu, A comprehensive review on latent heat and thermal conductivity of nanoparticle dispersed phase change material for low-temperature applications, Energy Storage Mater. 24 (2020) 52–74.
[30] H. Babar, H.M. Ali, Towards hybrid nanofluids: preparation, thermophysical properties, applications, and challenges, J. Mol. Liq. 281 (2019) 598–633.
[31] H. Ali, T.R. Shah, H. Babar, A.M. Ali, Hybrid nanofluids: Techniques and challenges of stability enhancement, in: 4Th Int Conf Adv Mech Eng Istanbul, 2018: pp. 60–76.
[32] T.-P. Teng, C.-C. Yu, Characteristics of phase-change materials containing oxide nano-additives for thermal storage, Nanoscale Res. Lett. 7 (2012) 611.
[33] Merck sigma aldrich, (n.d.). https://www.sigmaaldrich.com/.
[34] Nanostructured & Amorphous Materials, Inc., (n.d.). https://www.nanoamor.com/.
[35] Alfa Aesar, (n.d.). https://www.alfa.com/en/nanoparticles-tube-powder-etc/?page=2.
[36] H. Babar, H.M. Ali, Airfoil shaped pin-fin heat sink: potential evaluation of ferric oxide and titania nanofluids, Energy Convers Manag. 202 (2019).
[37] S. Sami, N. Etesami, Improving thermal characteristics and stability of phase change material containing TiO2 nanoparticles after thermal cycles for energy storage, Appl. Therm. Eng. 124 (2017) 346–352.
[38] TA Instruments, (n.d.). https://www.tainstruments.com/.
[39] A. Arshad, M. Jabbal, L. Shi, J. Darkwa, N.J. Weston, Y. Yan, Development of TiO2/RT–35HC based nanocomposite phase change materials (NCPCMs) for thermal management applications, Sustainable Energy Technol. Assess. 43 (2021).
[40] X. Zhang, C. Zhu, G. Fang, Preparation and thermal properties of n-eicosane/nano-SiO2/expanded graphite composite phase-change material for thermal energy storage, Mater. Chem. Phys. 240 (2020).
[41] T.M. Keller, S.B. Qadri, C.A. Little, Carbon nanotube formation in situ during carbonization in shaped bulk solid cobalt nanoparticle compositions, J. Mater. Chem. 14 (2004) 3063–3070.
[42] A.M. Taggart, F. Voogt, G. Clydesdale, K.J. Roberts, An examination of the nucleation kinetics of n-alkanes in the homologous series C13H28 to C32H66, and their relationship to structural type, associated with crystallization from stagnant melts, Langmuir 12 (1996) 5722–5728.
[43] M.J. Oliver, P.D. Calvert, Homogeneous nucleation of n-alkanes measured by differential scanning calorimetry, J. Cryst. Growth 30 (1975) 343–351.
[44] S. Harikrishnan, S. Magesh, S. Kalaiselvam, Preparation and thermal energy storage behaviour of stearic acid–TiO2 nanofluids as a phase change material for solar heating systems, Thermochim Acta 565 (2013) 137–145.

[45] H. Tian, W. Wang, J. Ding, X. Wei, M. Song, J. Yang, Thermal conductivities and characteristics of ternary eutectic chloride/expanded graphite thermal energy storage composites, Appl. Energy 148 (2015) 87–92.
[46] S. Wu, D. Zhu, X. Zhang, J. Huang, Preparation and melting/freezing characteristics of Cu/paraffin nanofluid as phase-change material (PCM), Energy Fuel 24 (2010) 1894–1898.
[47] A. Arshad, M. Jabbal, Y. Yan, Thermophysical characteristics and application of metallic-oxide based mono and hybrid nanocomposite phase change materials for thermal management systems, Appl. Therm. Eng. 181 (2020).
[48] M. Chieruzzi, A. Miliozzi, T. Crescenzi, L. Torre, J.M. Kenny, A new phase change material based on potassium nitrate with silica and alumina nanoparticles for thermal energy storage, Nanoscale Res. Lett. 10 (2015) 1–10.
[49] B. Dudda, D. Shin, Effect of nanoparticle dispersion on specific heat capacity of a binary nitrate salt eutectic for concentrated solar power applications, Int. J. Therm. Sci. 69 (2013) 37–42.
[50] T. Kozlowski, Modulated Differential Scanning Calorimetry (MDSC) studies on low-temperature freezing of water adsorbed on clays, apparent specific heat of soil water and specific heat of dry soil, Cold Reg. Sci. Technol. 78 (2012) 89–96.
[51] J. Wang, H. Xie, Z. Xin, Y. Li, L. Chen, Enhancing thermal conductivity of palmitic acid based phase change materials with carbon nanotubes as fillers, Sol. Energy 84 (2010) 339–344.
[52] X. Chen, P. Cheng, Z. Tang, X. Xu, H. Gao, G. Wang, Carbon-based composite phase change materials for thermal energy storage, transfer, and conversion, Adv. Sci. 8 (2021) 2001274.